Supporting Information

Open-air synthesis of oligo(ethylene glycol)-functionalized polypeptides from non-purified *N*-carboxyanhydrides

Zhengzhong Tan[1,‡], Ziyuan Song[1,‡], Tianrui Xue[2], Lining Zheng[1], Lei Jiang[1,3], Yunjiang Jiang[1], Zihuan Fu[2], Anh Nguyen[4], Cecilia Leal[1], and Jianjun Cheng [1,2,5-7]*

[1] Department of Materials Science and Engineering, University of Illinois at Urbana-Champaign, Urbana, Illinois 61801, United States.

[2] Department of Chemistry, University of Illinois at Urbana-Champaign, Urbana, Illinois 61801, United States.

[3] State Key Laboratory of Natural Medicines, Department of Pharmaceutics, China Pharmaceutical University, Nanjing 210009, China.

[4] Department of Chemical and Biomolecular Engineering, University of Illinois at Urbana-Champaign, Urbana, Illinois 61801, United States.

[5] Beckman Institute for Advanced Science and Technology, University of Illinois at Urbana-Champaign, Urbana, Illinois 61801, United States.

[6] Department of Bioengineering, University of Illinois at Urbana-Champaign, Urbana, Illinois 61801, United States.

[7] Materials Research Laboratory, University of Illinois at Urbana-Champaign, Urbana, Illinois 61801, United States.

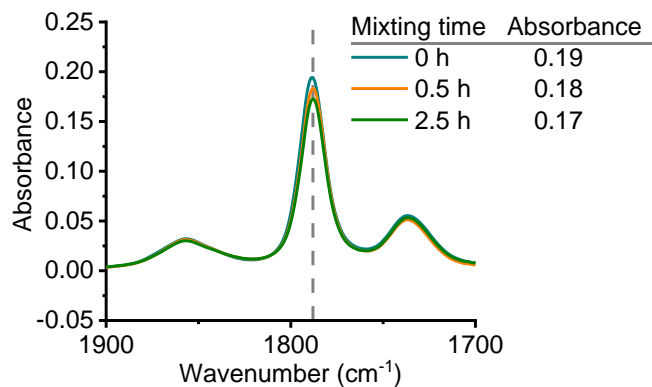[‡] These authors contributed equally; *Email: jianjunc@illinois.edu

Supporting Figures

Figure S1. FTIR study of partition of EG$_3$Glu NCA in water-in-oil emulsion (12% water). FTIR was performed on CHCl$_3$ phase before and at predetermined time intervals after water mixing. The dashed line indicates the characteristic peak of anhydride on NCA at 1788 cm^{-1}. The absorbance was used to quantify the amount of NCA in the CHCl$_3$ phase.
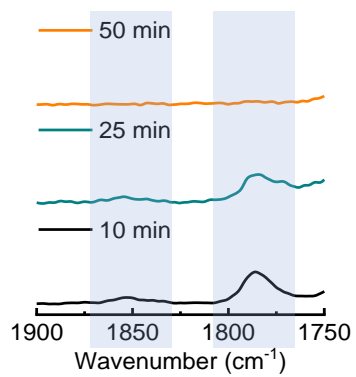
Figure S2. FTIR study of polymerization kinetics of EG$_3$Glu NCA in emulsion polymerization. The shadowed area indicates the decreasing of anhydride peaks during polymerization.
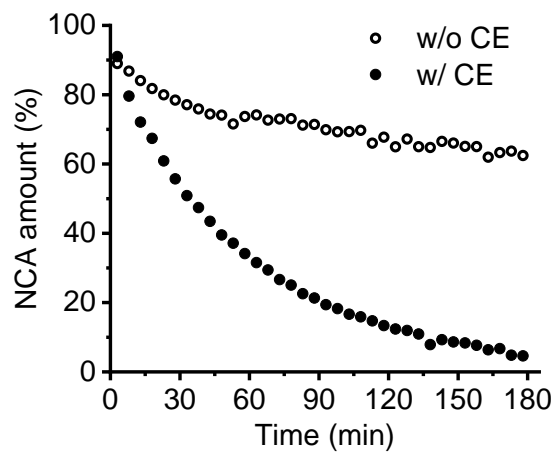
Figure S3. NMR study of polymerization kinetics of non-purified EG_3Glu-NCA in the biphasic system initiated by $PZLL-NH_2$ with (solid dot) and without CE catalysis (open dot).
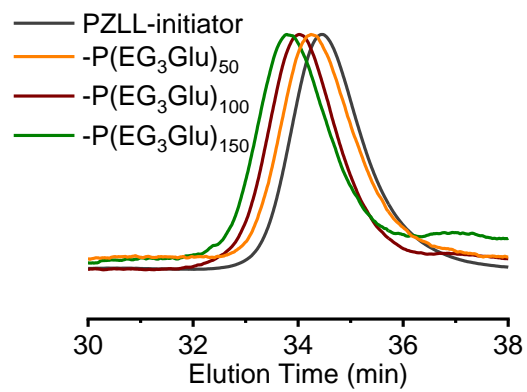
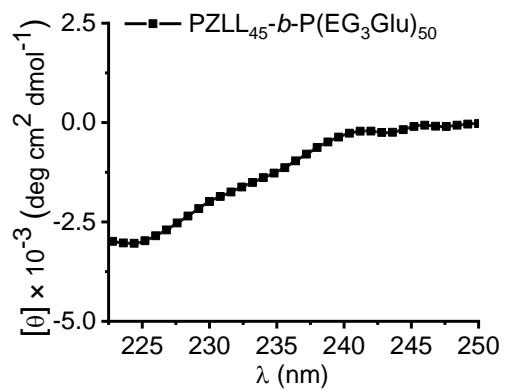Figure S4. GPC curves of PZLL initiator and PZLL-*b*-P(EG₃Glu) copolypeptides with different M/I ratio.

Figure S5. CD spectrum of PZLL$_{45}$-*b*-P(EG$_3$Glu)$_{50}$ in chloroform (0.1 mg/mL)
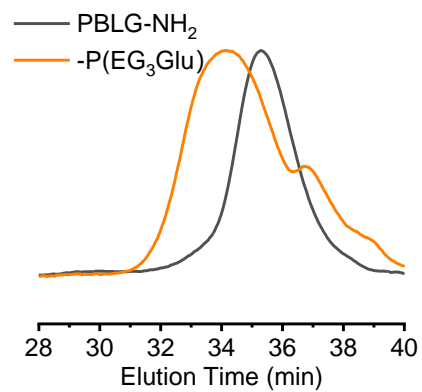
Figure S6. GPC curves of PBLG-initiator and resulting block copolypeptides PBLG-*b*-P(EG$_3$Glu). For the PBLG-*b*-P(EG$_3$Glu), Mn = 15.7 kDa, Đ = 1.17, DP (of EG$_3$Glu block) = 22.
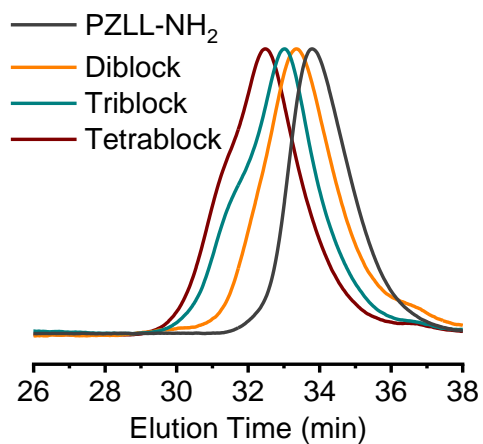
Figure S7. GPC curves of PZLL-initiator and multiblock polypeptides. Diblock: PZLL-*b*-P(EG₃Glu); triblock: PZLL-*b*-P(EG₃Glu)-*b*-PBLG; tetrablock PZLL-*b*-P(EG₃Glu)-*b*-PBLG-*b*-P(EG₃Glu).
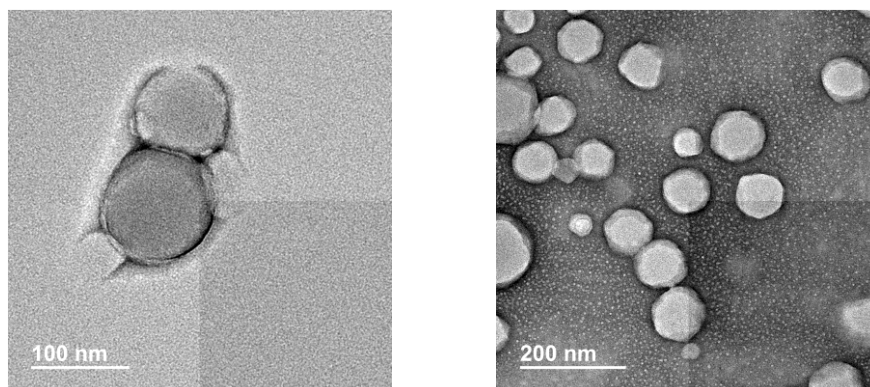
Figure S8. TEM images of PZLL$_{45}$-*b*-P(EG$_3$Glu)$_{150}$ (left) and PZLL$_{45}$-*b*-P(EG$_3$Glu)$_{100}$ (right).
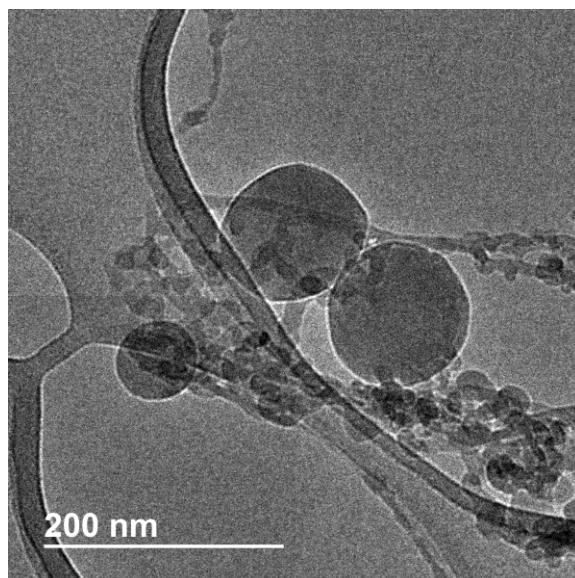
Figure S9. Cryo-TEM images of PZLL$_{45}$-*b*-P(EG$_3$Glu)$_{150}$ nanoparticles.
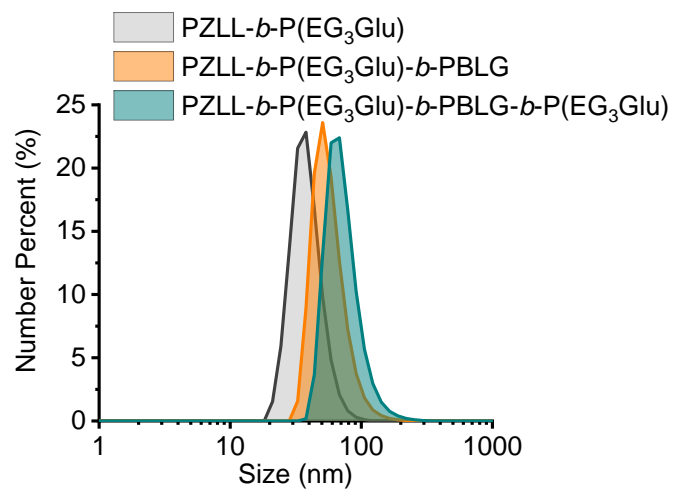
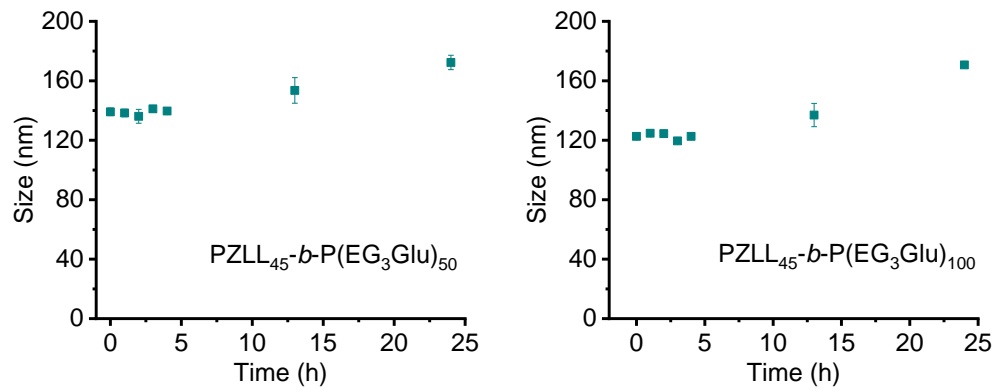Figure S10. DLS study of nanoparticle formed by multiblock copolypeptides.

Figure S11. Serum stability study of PZLL$_{45}$-*b*-P(EG$_3$Glu)$_{50}$ (left) and PZLL$_{45}$-*b*-P(EG$_3$Glu)$_{100}$ (right) nanoparticles.
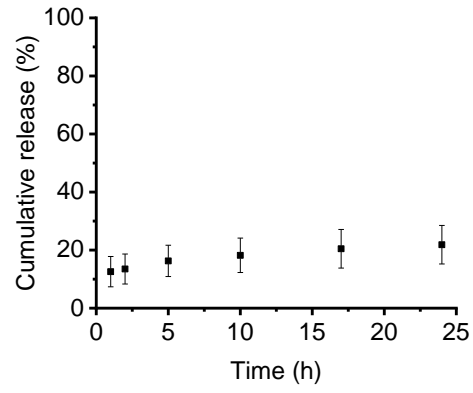
Figure S12. The cumulative release of PTX from PTX-loaded $PZLL_{45}$-b-$P(EG_3Glu)_{100}$ nanoparticle and. Error bar represents the standard deviation from three independent tests.
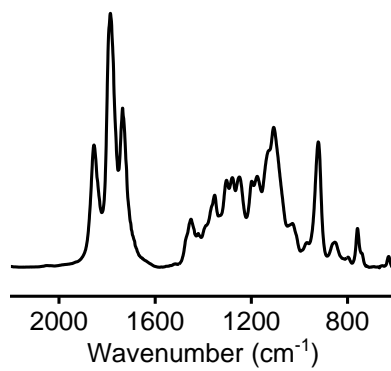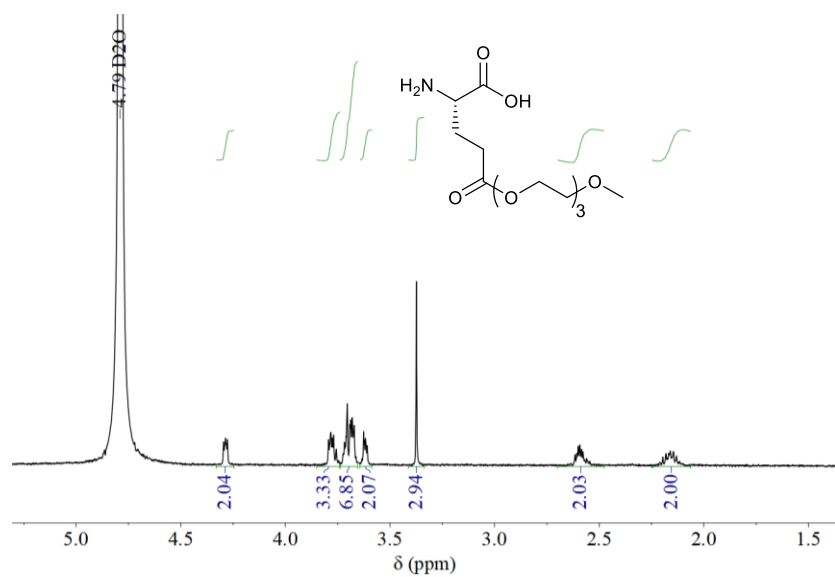
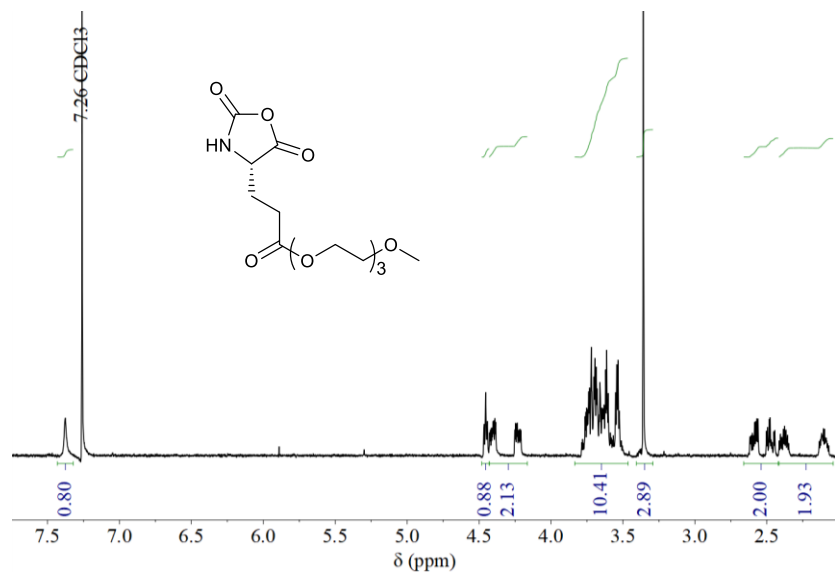Figure S13. FTIR spectra of EG$_3$Glu-NCA.

NMR Spectra

Figure S14. ^{1}H-NMR of EG$_{3}$Glu.

Figure S15. ^{1}H-NMR of EG$_3$Glu-NCA.

Figure S16. ^{1}H-NMR of PZLL-*b*-P(EG$_3$Glu).
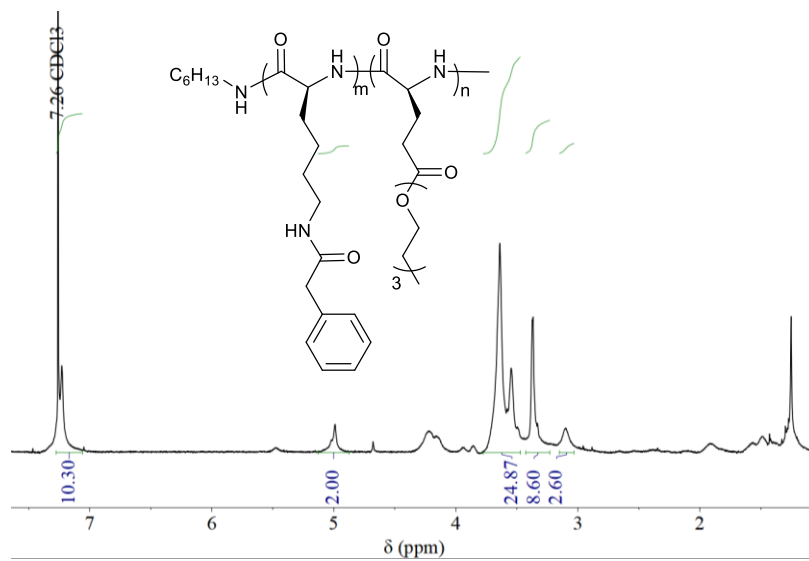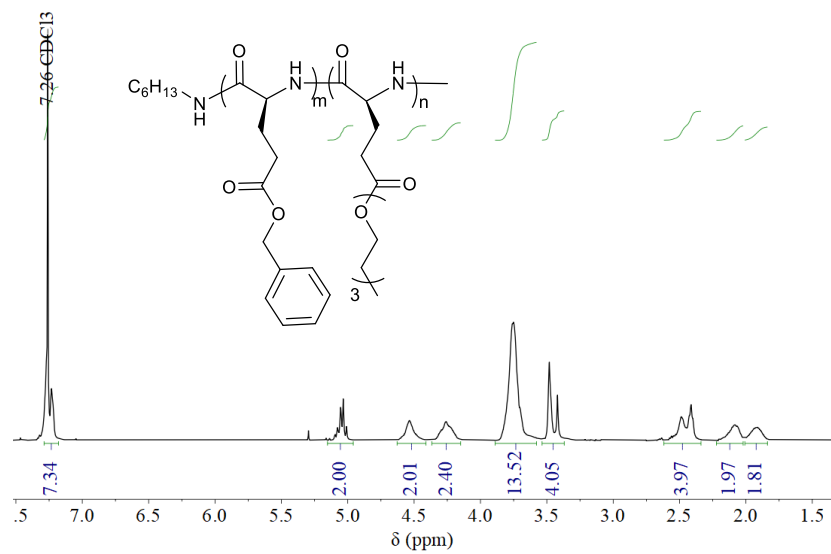
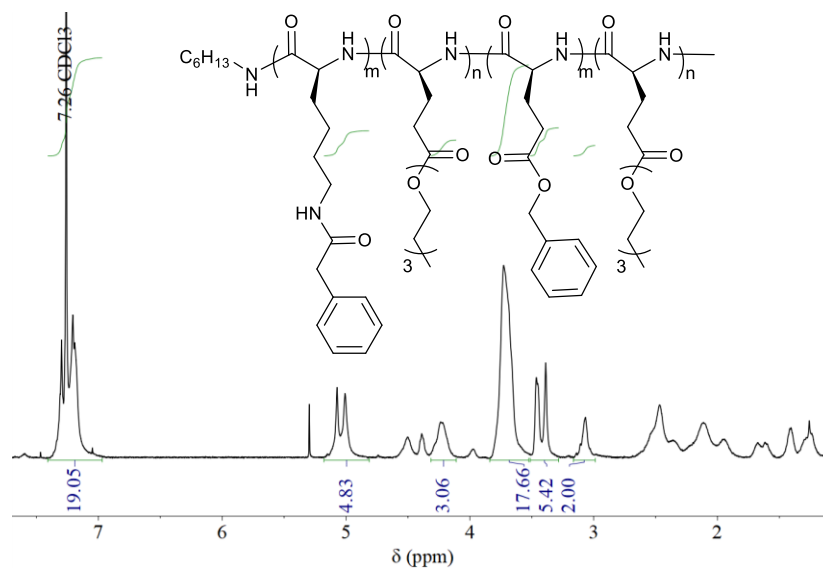Figure S17. ^{1}H-NMR of PBLG-*b*-P(EG$_3$Glu).

Figure S18. ^{1}H-NMR of PZLL-*b*-P(EG$_3$Glu)-*b*-PBLG-*b*-P(EG$_3$Glu).